

LINEAR OPTICS MEASUREMENT FOR THE APS RING WITH TURN-BY-TURN BPM DATA *

X. Huang[†], V. Sajaev, Y. P. Sun, A. Xiao, Argonne National Laboratory, Lemont, USA

Abstract

We measure the linear optics of the APS storage ring [1,2] from turn-by-turn BPM data taken when the beam is excited with an injection kicker. Decoherence due to chromaticity and amplitude-dependent detuning is observed and compared to theoretic predictions. Independent component analysis is used to analyze the data, which separates the betatron normal modes and synchrotron motion, despite contamination of bad BPMs. The beta functions and phase advances are subsequently obtained. The method is used to study the linear optics perturbation of an insertion device.

INTRODUCTION

Linear optics measurement and correction are critical for the operation of storage rings as the optics errors can degrade the nonlinear dynamics performance of the machines. Turn-by-turn (TBT) beam-position monitor (BPM) data taken when the beam is undergoing coherent betatron oscillation contain information about the linear optics. Simultaneous TBT BPM data on multiple BPMs can be analyzed with principal component analysis (PCA) [3] or independent component analysis (ICA) [4] methods.

In this study, we applied the ICA method to analyze TBT BPM data taken from the APS storage ring, from which we derived the beta functions and phase advances. The BPM noise and the resolution of the phase advance measurement are discussed. Decoherence due to chromaticity and amplitude-dependent detuning can significantly limit the number of usable turns in the TBT data. This was studied for the APS ring, where the impact is significant.

Changes were made to a quadrupole magnet to test the capability of resolving the linear optics errors. The method was also used to study the optics distortion due to an insertion device in the ring.

TBT BPM DATA OVERVIEW

The APS ring has 280 turn-by-turn BPMs distributed in the arcs of its 40 sectors. In the experiments we used the IK3 injection kicker to excite coherent oscillations in the horizontal plane. Since there is no vertical pinger, the linear coupling was increased slightly to introduce motion in the vertical plane.

Singular value decomposition (SVD) was used to estimate the BPM noise level, by constructing the noise with the 40 (out of 560) leading SVD modes removed. The results are shown in Fig. 1. The noise sigmas are 20 ~ 100 μm , with an average value of 50 μm for both planes. Also plotted in the

figure are the rms x and y readings from the first 100 turns, which indicate the size of the coherent oscillation.

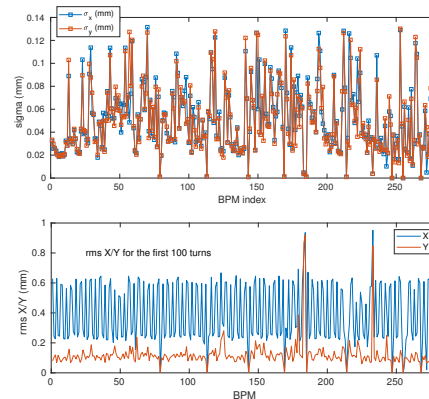


Figure 1: Top: BPM noise sigma estimated using data reconstructed without the first 40 singular values (out of 560). Bottom: rms x and y for the first 100 turns with IK3 voltage at 0.5 kV. Bad BPMs can be seen on the plots.

When the ICA method is applied to the TBT BPM data, the synchrotron motion can be separated from the beam motion. Figure 2 shows the temporal pattern and a portion of the spatial pattern of the synchrotron mode. The synchrotron tune, determined with NAFF [5], was found to be $\nu_s = 0.00802$. By comparing the spatial pattern to the model dispersion, the energy oscillation amplitude is determined to be $\delta_m = 0.12 \times 10^{-3}$.

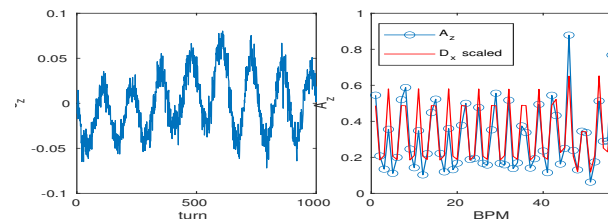


Figure 2: The temporal pattern (left) and the spatial pattern of 1/8 of the ring (right) of the ICA mode for longitudinal motion. The temporal vector is normalized to $\|s\| = 1$.

DECOHERENCE

The APS ring routinely operates with high chromaticities to suppress collective instabilities [6]. It is well known that a kicked beam bunch will decohere, causing the centroid motion seen by BPMs to decrease [7]. Second order chromaticities and amplitude-dependent detuning also introduce additional decoherence effects [8]. In the APS data, we took systematic measurements to characterize the decoherence effects from both chromaticity and amplitude detuning.

* Work supported by DOE Contract No. DE-AC02-06CH11357

[†] huangxb@anl.gov

Figure 3 shows the temporal pattern of the horizontal betatron mode for two chromaticity levels ($C_x = 5.4$ or 1.4) and three kicker voltage levels (IK3=1, 0.5, or 0.25 kV). There were 8 consecutive bunches with bunch charges at 0.5 nC in the ring. We neglect the head-tail damping due to impedance as the beam current is low.

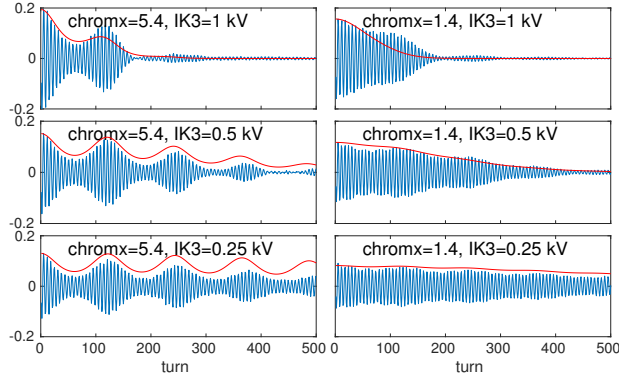


Figure 3: Temporal pattern with three levels of kicker voltage and two chromaticities. Bunch charge is 0.5 nC. Red curves are theoretic predictions.

Using formulas given in Ref. [7, 8], the decrease of the beam centroid oscillation amplitude can be predicted. In Fig. 3 the theoretic predictions are also plotted, using parameters calculated by an ideal lattice (listed in Table 1). The effects of linear, nonlinear chromaticities, and amplitude detuning are included. The initial kick is determined by comparing the amplitude measurements at all BPMs to the calculated beta functions. The decoherence pattern could serve as an way to probe the beam distribution.

Table 1: Lattice Parameters for Decoherence Calculation

C_{x2}	$\sigma_\delta (\times 10^{-3})$	$\frac{dv_x}{dJ_x} \frac{10^3}{m}$	ϵ_x nm
70.6	0.96	-34.6	2.7

LINEAR OPTICS MEASUREMENT

Beta Functions and Phase Advances

Using the pair of ICA betatron modes for the motion in each plane, the beta functions and phase advances can be calculated. Figure 4 shows the measured beta functions and phase advances for one data set (with chromaticities $C_x = 3.4$ and $C_y = 3.8$, IK3 = 0.5 kV) as an example. The measured beta functions are impacted by BPM calibration errors. However, the phase advances are not affected as they are determined by the ratio of the two spatial modes. The standard deviation of the ψ_x difference between the measurement and the model is 36.8 mrad.

Three data sets were taken for the same condition, from which the uncertainty levels of phase advance measurements may be estimated. Figure 5 shows the differences of the

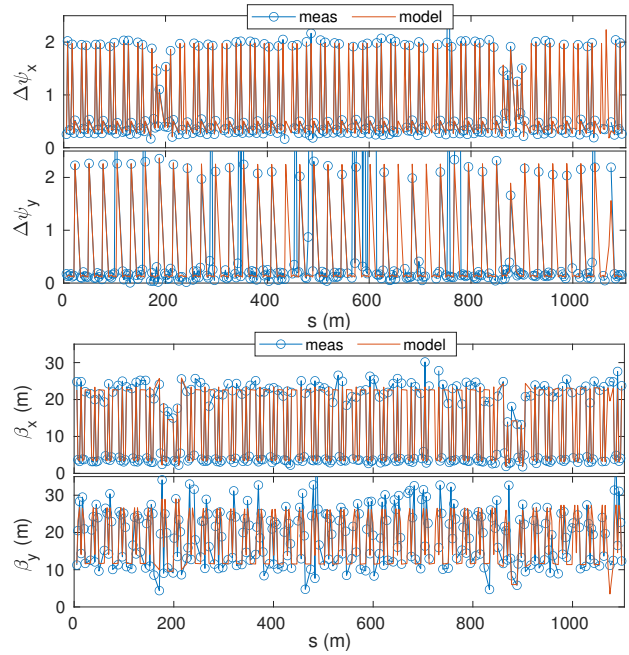


Figure 4: (top) Phase advances increments between BPMs; (bottom): beta functions. Measurements are compared to lattice model.

measured phase advances between two data sets and the third set. The error sigmas for measured $\psi_{x,y}$ are 18 mrad (H) and 74 mrad (V), respectively, consistent with the signal to noise ratios.

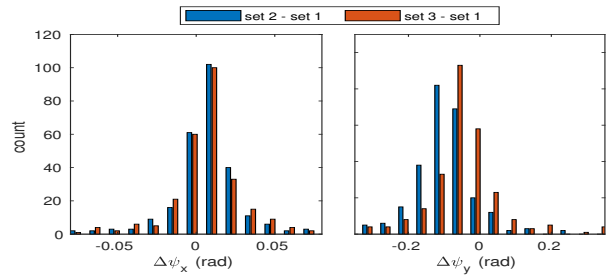


Figure 5: Differences of measured $\psi_{x,y}$ in three data sets.

Changes Due to One Quadrupole

To test the ability to measure linear optics errors with TBT BPM data, we deliberately changed one quadrupole in the ring and took data for comparison. In the experiment, we varied the quadrupole (S10A:Q2) by -1% and -2% , from its original set point.

Figure 6 shows the differences of measured phase advances between the cases with or without the changes on the magnet. The changes predicted by the lattice model are also potted for comparison. The measured changes closely follow the model predictions, with a scaling error of about 25%, which could be due to hysteresis.

OPTICS PERTURBATION BY AN ID

TBT BPM data were used to characterize the perturbation to the APS linear optics by an electromagnetic wiggler

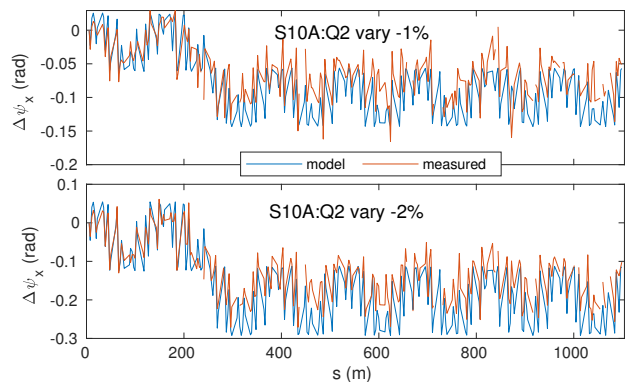


Figure 6: Measured horizontal phase advance changes with quadrupole S10A:Q2 (located at $s = 253$ m) setpoint changed by -1% (top) and -2% (bottom). Model values are plotted for comparison.

(IEX) [9]. This device has a strong impact on the optics, which is compensated with nearby quadrupoles through a feed-forward table [10]. In this study, we took TBT BPM data with the ID powered at different levels, with feed-forward on or off.

Figure 7 shows the horizontal phase advance changes due to the IEX in the vertically deflecting mode as measured with TBT BPM data. The ID is located at $s = 800.4$ m. When the feed-forward is off, the optics distortion is significant. The measurement also shows that the feed-forward properly cancels the perturbation by the ID.

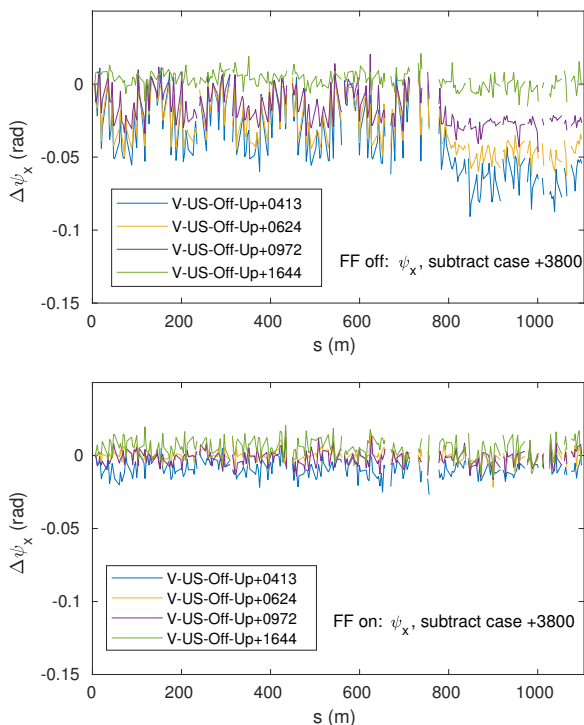


Figure 7: Measured horizontal phase advance changes due to the IEX wiggler, with feed-forward off (top) or on (bottom).

By fitting the measured linear optics functions to the lattice model, optics correction can be achieved [4, 11]. As a special case, the linear optics measurements by the TBT BPM can be used to determine the feed-forward table. The quadrupole triplets on both sides of the ID are used. Because changes to the quadrupoles are expected to be small, the combined optics perturbation can be considered a linear superposition. In a simplified approach, the least-square fitting problem can be defined with

$$f(\mathbf{p}) = \chi^2 = \sum_i \frac{1}{\sigma_{\psi_{x,i}}^2} \left(\Delta\psi_{x,i}^{\text{meas}} - \sum_j^{N_q} \frac{d\psi_{x,i}}{dK_j} p_j \right)^2 + \frac{1}{\sigma_{\nu_x}^2} \left(\Delta\nu_x^{\text{meas}} - \sum_j^{N_q} \frac{d\nu_x}{dK_j} p_j \right)^2 + \text{+y-terms}, \quad (1)$$

where $\frac{d\psi_{x,i}}{dK_j}$ is calculated with the lattice model and the fitting parameters \mathbf{p} are quadrupole gradient changes.

The fitting method takes only one step to find the solution. Figure 8 shows the residual vector before and after fitting for one case.

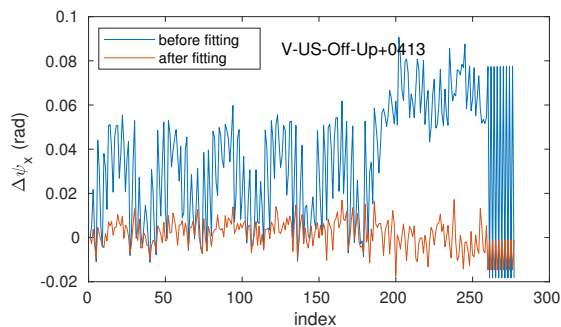


Figure 8: Phase advance errors before and after fitting for one ID mode (“Up + 0413”).

SUMMARY

Turn-by-turn BPM data are used to characterize the linear optics of the APS storage ring. The ICA method is used to separate the betatron modes and synchrotron mode, from which the linear optics functions are determined [4]. The decoherence of a kicked beam due to linear and second order chromaticities and amplitude-dependent detuning are observed and modeled with theory [7, 8]. The method is used to study the linear optics perturbation of an insertion device and to determine the required changes to nearby quadrupoles for optics correction.

REFERENCES

- [1] J. Galayda, “The advanced photon source”, in *Proc. PAC’95*, Dallas, TX, USA, May 1995, paper MAD02, pp. 4–8.
- [2] L. Emery, M. Borland, R. Dejus, E. Gluskin, and E. Moog, “Progress and prospects toward brightness improvements at the advanced photon source”, in *Proc. PAC’01*, Chicago, Illinois, USA, Jun. 2001, paper WPPH065, pp. 2602–2604.

- [3] C.-x. Wang, V. Sajaev, and C.-Y. Yao, “Phase advance and function measurements using model-independent analysis”, *Phys. Rev. ST Accel. Beams*, vol. 6, p. 104001, Oct. 2003. doi:10.1103/PhysRevSTAB.6.104001
- [4] X. Huang, S. Y. Lee, E. Prebys, and R. Tomlin, “Application of independent component analysis to fermilab booster”, *Phys. Rev. ST Accel. Beams*, vol. 8, p. 064001, Jun. 2005. doi:10.1103/PhysRevSTAB.8.064001
- [5] J. Laskar, C. Froeschlé, and A. Celletti, “The measure of chaos by the numerical analysis of the fundamental frequencies. application to the standard mapping”, *Physica D: Nonlinear Phenomena*, vol. 56, no. 2, pp. 253–269, 1992. doi:10.1016/0167-2789(92)90028-1
- [6] R. R. Lindberg and A. Blednykh, “Instability thresholds for the advanced photon source multi-bend achromat upgrade”, in *Proc. IPAC’15*, Richmond, VA, USA, May 2015, pp. 1822–1824. doi:10.18429/JACoW-IPAC2015-TUPJE077
- [7] R. Meller, A. Chao, J. Peterson, S. Peggs, and M. Furman, “Decoherence of kicked beams”, Superconducting Super Collider laboratory, Dallas, Texas, USA, Rep. SSC-N-360, 1987.
- [8] S. Lee, “Decoherence of the kicked beam ii”, Superconducting Super Collider laboratory, Dallas, Texas, USA, Rep. SSC-N-749, 1991.
- [9] M. S. Jaski *et al.*, “An Electromagnetic Variably Polarizing Quasi-Periodic Undulator”, in *Proc. North American Particle Accelerator Conf. (NAPAC’13)*, Pasadena, CA, USA, Sep.-Oct. 2013, paper WEPSM09, pp. 1064–1066.
- [10] A. Xiao *et al.*, “The Intermediate-Energy X-ray (IEX) Undulator Commissioning Results”, in *Proc. North American Particle Accelerator Conf. (NAPAC’13)*, Pasadena, CA, USA, Sep.-Oct. 2013, paper WEPSM11, pp. 1070–1072.
- [11] X. Yang and X. Huang, “A method for simultaneous linear optics and coupling correction for storage rings with turn-by-turn beam position monitor data”, *Nuclear Instruments and Methods in Physics Research Section A: Accelerators, Spectrometers, Detectors and Associated Equipment*, vol. 828, pp. 97–104, 2016. doi:10.1016/j.nima.2016.05.020